24th COBEM - 2017

24th ABCM International Congress of Mechanical Engineering
December 3-8, 2017, Curitiba, PR, Brazil

COBEM-2017-0477
EXPERIMENTAL CHARACTERIZATION OF THE NONLINEAR CHARACTERISTICS OF FRICTION IN PNEUMATIC ACTUATORS

Roger Oliva Felix
Marcos Silveira
School of Engineering - UNESP - Bauru/SP, Brazil, End.: Av. Eng. Luiz Ed. Carrijo Coube 14-01, CEP. - 17033-360, Fone - 55 14 3103-6000
roger.felix@feb.unesp.br, m.silveira@feb.unesp.br

Abstract. *This paper presents an experimental procedure for determination of the nonlinear characteristics of internal friction of pneumatic actuators. Pneumatic actuators are a clean technology compared to hydraulic actuators, have good relationship between power and supported mass, and low cost compared to electric actuators. They also have nonlinear characteristics which influence the control, and in order to get the positioning accuracy it is necessary a good characterization of internal friction. This paper consists of the investigation of parameter sensibility of LuGre friction model using an experimental rig with a low cost controller, and finally to perform experimental tests with automatic identification of friction in pneumatic actuators, with graphical display of static and dynamic parameters. The force of friction in relation to model parameters is calculated in real time, enabling the visualization of behaviour of the pneumatic actuator.*

keywords: *experimental characterization of friction, low cost controller, pneumatic actuator*

1. INTRODUCTION

The study of friction in pneumatic actuators is related to a difficulty of control in positioning systems. The actuator internal friction is function of the displacement of the piston in contact with the inner surface. This contact between the piston and the surface exists for preventing pressure drop or leak.

There are several friction models, such as, static, viscous, Coulomb, Stribeck, Dahl and LuGre model, among others. Each friction model has different characteristics, which can affect the positioning system in an industrial control system.

The actuator is designed to work with pressures between its internal chambers, it has a seal between the piston and the surface in order to not have pressure drop or leakage. De Wit *et al.* (1995) proposed a new dynamic model for friction, denominated LuGre model, based on average bending of recesses existing between the contact materials, as shown in Fig. 1. This model is widely used in nonlinear systems for friction compensation. Through the identification of internal friction in a pneumatic actuator it is possible to develop a control system of compensation (Andrighetto *et al.*, 2006).

Many experimental methods have been proposed to investigate the friction characteristics in pneumatic actuators. Schroeder and Singh (1993) proposed an experimental test in which the friction force was calculated by detecting the force exerted by the rods of the tested pneumatic actuator and of a load pneumatic actuator assembled with a reversed working direction. Belforte *et al.* (2003) proposed an experimental test in which the velocity of the test pneumatic actuator was controlled by a driving hydraulic actuator and the pressures of the chambers were controlled by proportional pressure control valves in order to measure the friction force under a broad range of operating conditions of velocity and pressures. Nouri (2004) proposed an experimental test to identify the friction force in both the presliding and sliding regimes. However, all these experimental methods focused mainly on investigating the steady state friction characteristics. Chang *et al.* (2012) performed the study of comparison of the friction force on pneumatic actuators with grease and dry lubrication, in which the lubrication sealing system had a significant reduction in the friction force.

The objective of this paper is to perform an analysis of the static and dynamic behaviour of pneumatic actuators and identify the characteristics of the friction of the actuator utilising an automatic process using a low cost experimental rig. This characterization procedure may be useful to many precision pneumatic systems applied in industrial processes.

2. LUGRE MODEL

The LuGre friction model has been accepted as an accurate model that can describe the real friction phenomenon in most experiments. In the model, the friction contact surface is identified as a group of elastic bristles with random behaviour in the micro scale. The friction is generated by the deflection of bristles.

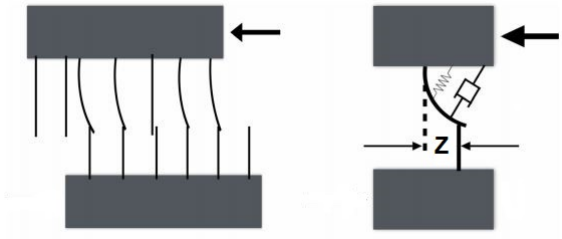

Figure 1. Contact area between two surface and average deflection between the contact area is represented by z - Adapted from Sun *et al.* (2016)

The friction force is composed of three parts, in which the first refers to the average of the deformation $\sigma_0 z$, the second is proportional to the rate of change of the deformation $\sigma_1 \dot{z}$, and the third to the friction drag caused by the resistance to movement of the body through a fluid (Guenther *et al.*, 2006). The friction force caused by microdeformation z is given by

$$F_f = \sigma_0 z + \sigma_1 \dot{z} + \sigma_2 \dot{y}^2 \text{sgn}\,(\dot{y}) \tag{1}$$

in which F_f is the friction force, σ_0 is the stiffness coefficient of microdeformations, σ_1 is the damping coefficient, σ_2 is the drag coefficient, and sgn() is the sign function. The dynamics of microdeformation, characterised by the non measurable variable z, is modelled by Eq. (2), which is incorporated into the LuGre model:

$$\dot{z} = \dot{y} - a(z, \dot{y}) \frac{\sigma_0}{\text{g}_{ss}(\dot{y})} \|\dot{y}\| z \tag{2}$$

in which $a()$ is the function to get the static friction in low velocity, $\|\dot{y}\|$ is the absolute value of the velocity, and g_{ss} is the positive function of the characteristics of friction in steady state, given by

$$\text{g}_{ss}(\dot{y}) = F_c + (F_s - F_c) e^{-\left(\frac{\dot{y}}{\dot{y}_s}\right)} \tag{3}$$

in which F_c is the Coulomb friction, F_s is the static friction and $\dot{y}_s$ is the Stribeck velocity. Therefore, in steady state, $\dot{y}$ is constant, and $a(z, \dot{y}) = 1$ and $\dot{z} = 0$ (Johanastrom and Canudas-de Wit, 2008). Substituting these values in Eq. (1), it is possible to identify the parameters of static friction (F_c, F_s, σ_2 e $\dot{y}$), as follows

$$F_f = \text{sgn}(\dot{y})(F_c + (F_s - F_c)) e^{-\left(\frac{\dot{y}}{\dot{y}_s}\right)^2} + \sigma_2 \dot{y}^2 \text{sgn}\,(\dot{y}) \tag{4}$$

With this description, the LuGre model is characterised by six parameters F_c, F_s, $\dot{y}$, σ_0, σ_1, and σ_2,. Among them, parameters such as F_c, F_s, $\dot{y}$ and σ_2 can be identified by the means of measuring the steady state friction of the pneumatic actuator when its velocity is held constant and Fig. 2 shows the curve of LuGre friction model. However, the identification of the dynamic parameters σ_0 and σ_1. The static parameters can be used to calculate the dynamic parameters using the methodology proposed by (Perondi *et al.*, 2002).

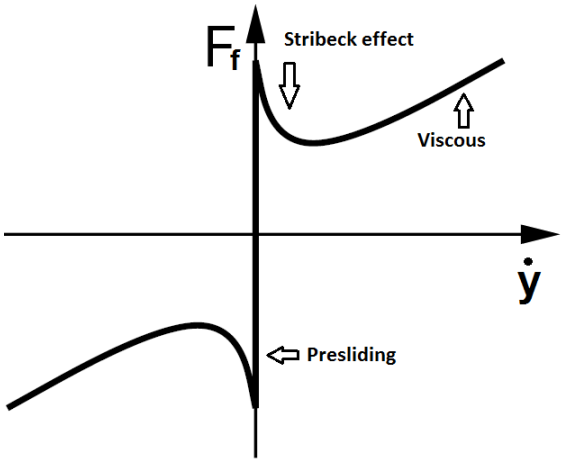

Figure 2. Curve of LuGre friction model - Adapted from (Ha *et al.*, 2006)

3. EXPERIMENTAL RIG

Figure 4 shows the experimental rig, built to perform the tests of friction in pneumatic actuators, using low cost controller Raspberry Pi and pneumatic instruments fixed at polypropylene plate.

The forces exerted on the piston are composed of the following forces: F_f is the friction force, which mainly occurs on the surfaces of contact between the rod and the seals, F_l is the amplitude of external load, and F_p is the pneumatic force. The dynamic equation is given by

$$M\ddot{y} + F_f = F_p - F_l \tag{5}$$

in which M refers to the mass of the piston with the rod and $\ddot{y}$ the acceleration to the displacement of the rod. The pneumatic force corresponds to the difference of pressure in the chambers of the actuator. When velocity is constant, the friction force is equal to the pneumatic force. The pneumatic force is given by

$$F_p = A_a P_a - A_b P_b \tag{6}$$

in which A_a, P_a, A_b, and P_b are respectively the chamber area a, pressure of the chamber a, chamber area b, and pressure of the chamber b. The static friction force is estimated by the minimum pressure needed to move the piston from zero velocity, and is given by

$$F_s = P_s A \tag{7}$$

in which P_s is the initial pressure for the displacement of piston and A is the chamber area. Table 1 shows the parameters of the pneumatic actuator (ISO6432 standard model), with double action and grease lubrication.

Table 1. Basic parameters of the actuator

Description	Symbol	Value
Diameter of piston	D	0.025 m
Diameter of rod	D_r	0.010 m
Stroke	L	0.300 m
Area of piston	A_a	4.909×10^{-4} m^2
Area (piston - rod)	A_b	4.123×10^{-4} m^2
Initial volume of chamber A	V_a	1.473×10^{-4} m^3
Initial volume of chamber B	V_b	1.237×10^{-4} m^3

The purpose of the electronic system is to perform the data acquisition of the variables in real time. Figure 5 shows the schematic diagram of pneumatic and electronic circuits, in which the Human Machine Interface (IHM) uses a touch screen to communicate with the controller Raspberry Pi 3. In order to acquire analog variables it was necessary to obtain an external electronic board with AD/DA (Analog-Digital and Digital-Analog) converters, with 24-bit AD and 16-bit DA of resolution. Figure 3-a shows the physical controller Raspberry Pi 3 and Fig. 3-b shows the board of converters AD/DA.

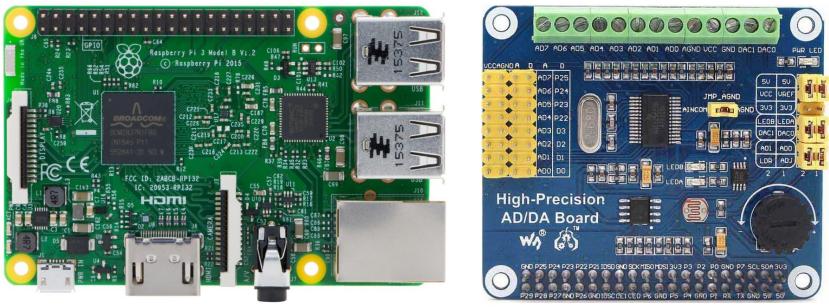

Figure 3. Raspberry Pi 3 controller - source: https://www.raspberrypi.org/ and converters AD/DA - source: http://www.waveshare.com

Figure 6 shows the module of the ultrasonic sensor used in the experimental rig is model HC-SR04, capable of measuring distances of 2 cm to 4 m with precision of 2 mm. This module has a ready circuit with emitter and receiver coupled and 4 pins (VCC, TRIGGER, ECHO, GND) for measurement. The equation for distance calculation is given by

$$d = \frac{t\,v}{2} \tag{8}$$

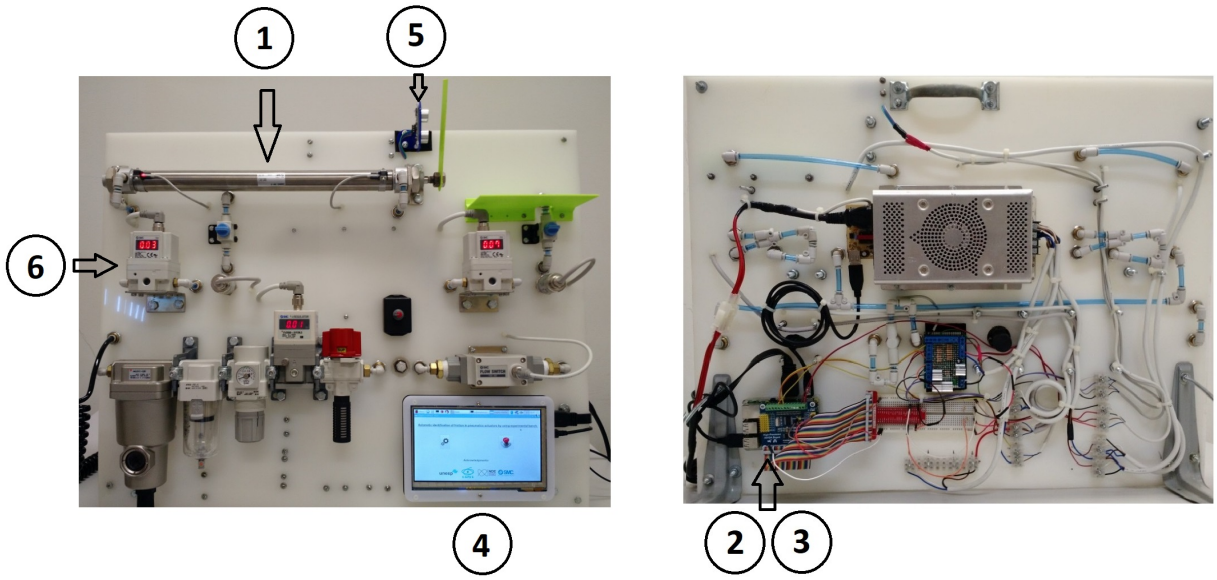

Figure 4. Experimental rig with front and back view

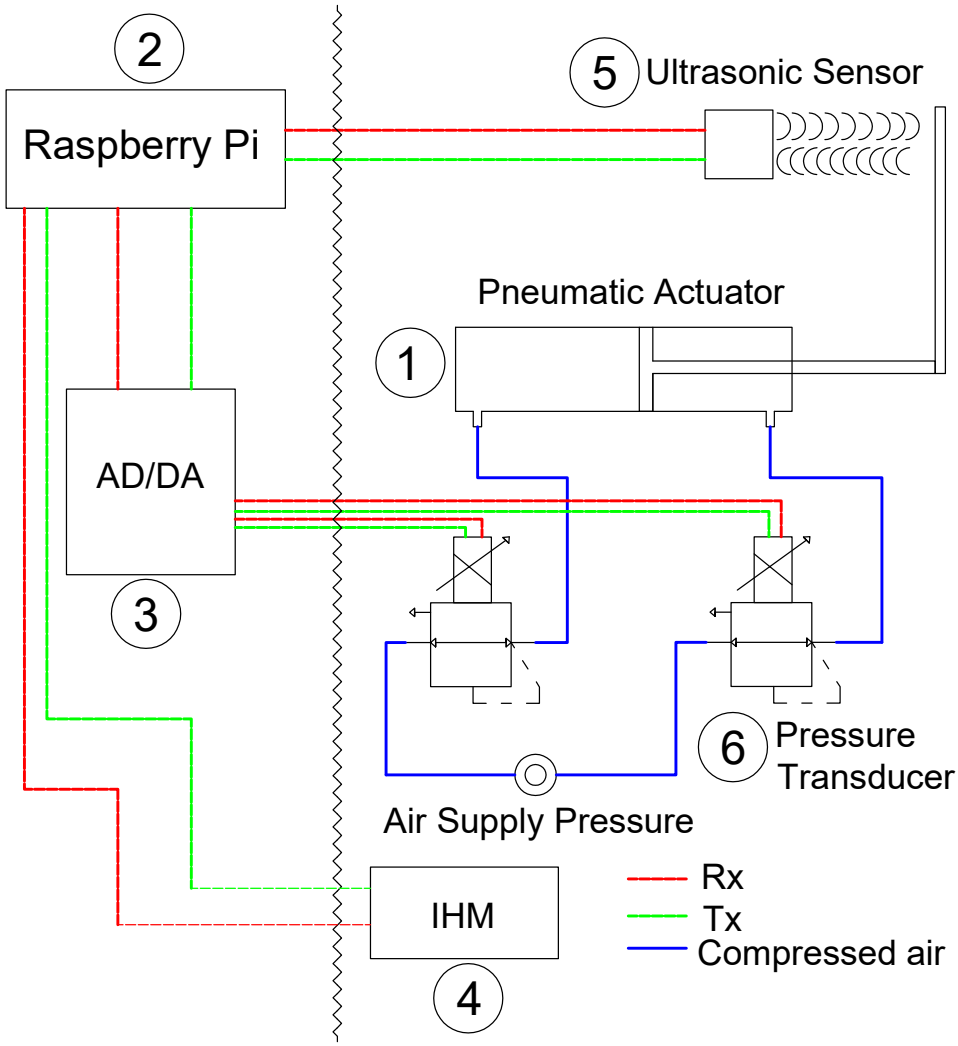

Figure 5. Schematic diagram of pneumatic and electronic circuits (Rx: receiver; Tx: transmission)

in which d is the distance, v is the speed of sound and t is the high level time on the ECHO pin. The speed of sound can be considered equal to 340 m/s. In the equation, the division by two is because the wave is sent and returned to the sensor.

Figure 6. Ultrasonic sensor

Figure 7 shows the main screen and setup for achievement of each experiment, the first button performs the settings of pressure for extension and compression, and second button starts the experiment.

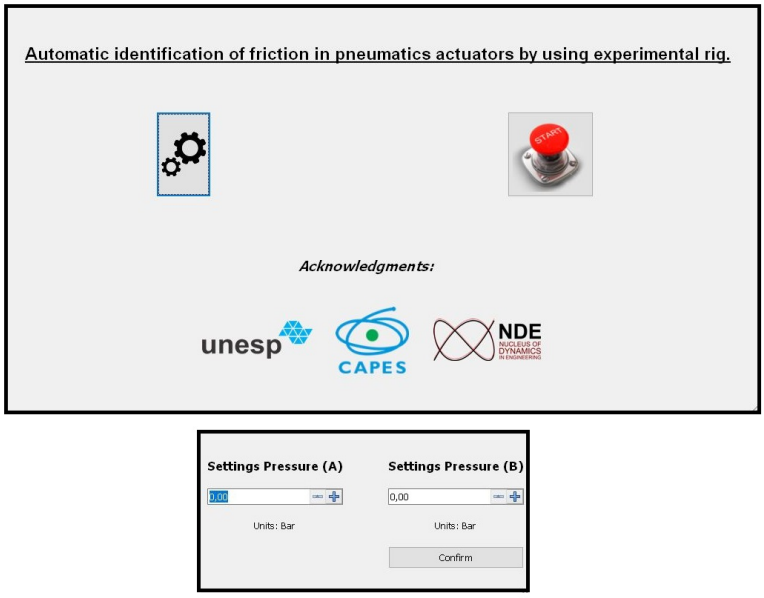

Figure 7. Interface of user in experimental rig

4. RESULTS

For the identification of the friction twenty experiments were performed varying the pressure of input of actuator and consequently changing the piston velocity in the expansion and compression. For each performed experiment, the time interval in which the velocity is constant was extracted, and a linear fit was performed, as shown in Fig. 8.

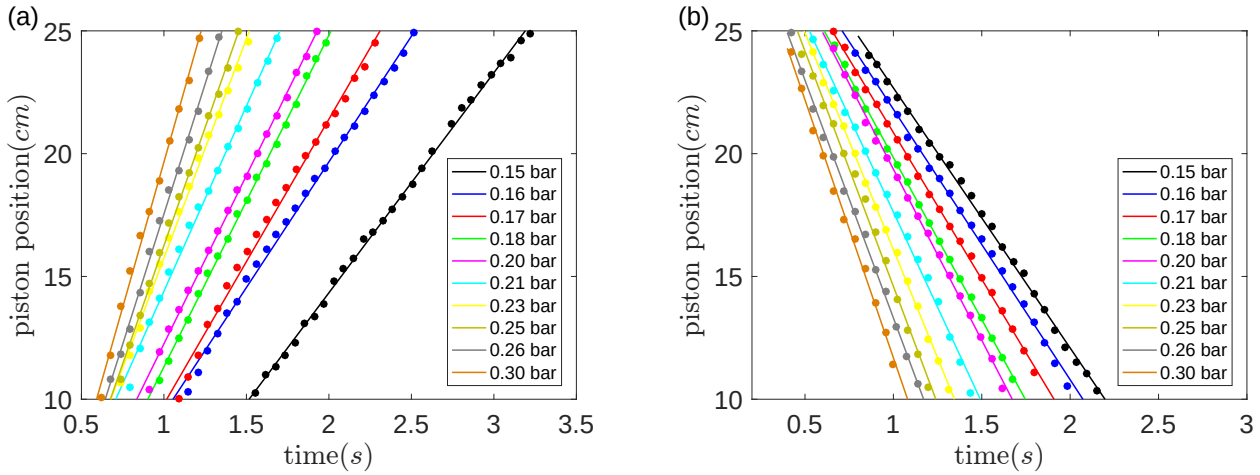

Figure 8. (a) Piston position as function of time, and respective linear fits for extension; (b) Piston position as function of time, and respective linear fits for compression. (• experimental results; – fits)

Table 2 shows the confidence intervals for each linear fit performed to find the parameters c_1 and c_2 of equation of the line ($c_1 x + c_2 = 0$), in which giving the minimum and maximum values of each parameter for extension and compression of the actuator.

Table 2. Confidence intervals of the linear regression

Confidence intervals for 95%								
$P_a - P_b$	**Extension**				**Compression**			
	c_1		c_2		c_1		c_2	
	minimum	**maximum**	**minimum**	**maximum**	**minimum**	**maximum**	**minimum**	**maximum**
0.15	8.8199	9.1035	-3.9337	-3.2446	-10.7912	-10.3907	32.9579	33.5788
0.16	9.9674	10.4941	-1.2899	-0.3027	-11.2591	-10.7656	32.4671	33.1707
0.17	11.1455	12.0596	-2.5872	-1.0147	-12.1155	-11.7810	32.5931	33.0204
0.18	13.2588	13.7485	-2.5551	-1.8172	-13.3505	-13.0188	32.8217	33.2234
0.20	13.3771	14.0387	-1.9314	-0.9716	-14.2210	-13.6372	32.9512	33.6380
0.21	14.4826	15.6745	-1.4365	0.0769	-16.0572	-14.9648	32.5751	33.6980
0.23	17.1942	18.5164	-2.8666	-1.3497	-17.9640	-17.3282	33.4368	34.0476
0.25	18.7008	19.8244	-3.6346	-2.3822	-20.0063	-18.2846	32.9934	34.4909
0.26	20.4255	21.9887	-4.4666	-2.8662	-20.0367	-18.6699	32.1107	33.2195
0.30	22.5062	24.8187	-5.0853	-2.9255	-22.0059	-20.0029	31.9476	33.4359

The pneumatic force is shown in Fig. 9, calculated using Eq. (6), which is dependent of pneumatic pressure measured by transducer of pressure and the chamber areas. The small variation contained in the friction force in each experimental test occurs due to the pressure regulating instrument. The pneumatic force for extension compared to compression has force different from each experimental test due to difference of chamber areas.

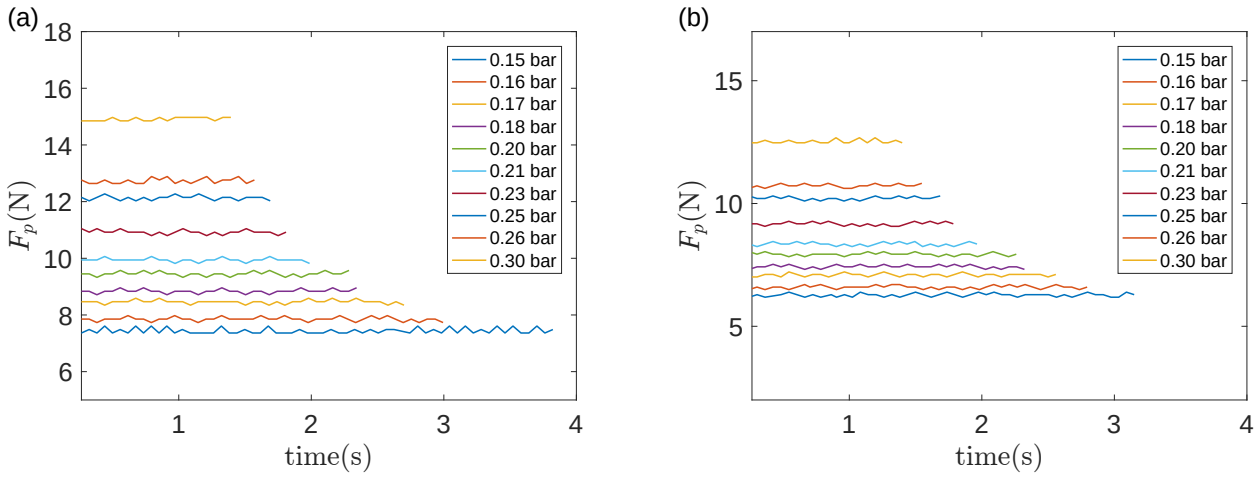

Figure 9. (a) Pneumatic force in function of time for extension; (b) Pneumatic force in function of time for compression

Figure 10 shows the map of static friction, the tests were performed in extension and compression of the pneumatic actuator with different chamber area ($A_a \neq A_b$) and without external load, identifying the friction force at positive velocities and negative, in which the first experimental point at zero velocity corresponds the static friction force calculated using of Eq. (7), and other points the average dynamic friction forces in the time interval which the velocity is constant. After the experimental tests, the parameters of the LuGre model were adjusted with the use of *nlinfit* function of *Matlab* software, which corresponds to a nonlinear regression of the experimental points to fit Eq. (4).

The friction force as function of velocity for extension and compression has the asymmetry mainly of the difference of chambers area of pneumatic actuator and others internal factors of actuator as wear of the seal of piston and absence of lubrication. About the static friction force has larger value for the extension compared to the compression.

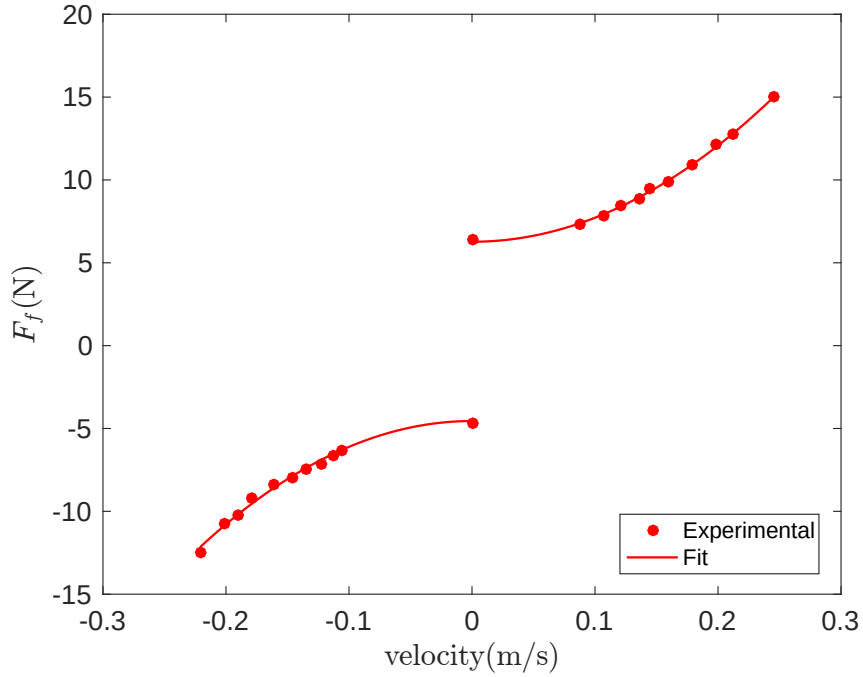

Figure 10. Friction force as function of velocity, and respective nonlinear fits. (• experimental results; – fits)

5. CONCLUSION

In this paper, the mathematical modelling and low cost experimental rig to identify nonlinear friction behaviour of a pneumatic actuator devices were shown. With the LuGre model described, the nonlinear characteristics of dynamic friction were studied, and through the map of static friction it is possible to analyse some characteristics of nonlinear friction finding the dynamic parameters with the nonlinear regression adjustment of the mathematical model. It was observed the asymmetry in the friction force as function of velocity and characterised mainly by difference of area of pneumatic actuator, the friction force behaviour has an asymmetry in different directions of velocity. Therefore, using low cost devices it was possible to identify the friction force of the pneumatic actuator. The next steps for completion of the research is to identify the dynamic parameters (σ_0 e σ_1) for negative velocities (compression) and positive velocities (extension).

6. ACKNOWLEDGEMENTS

The authors thank the Brazilian funding agency CAPES (Coordenação de aperfeiçoamento de pessoal de nível superior) for financial support for this project.

7. REFERENCES

Andrighetto, P.L., Valdiero, A.C. and Carlotto, L., 2006. "Study of the friction behavior in industrial pneumatic actuators". In *ABCM Symposium series in mechatronics*. Vol. 2, pp. 369–376.

Belforte, G., Mattiazzo, G., Mauro, S. and Tokashiki, L., 2003. "Measurement of friction force in pneumatic cylinders". *Lubrication Science*, Vol. 10, No. 1, pp. 33–48.

Chang, H., Lan, C.W., Chen, C.H., Tsung, T.T., Guo, J.B. *et al.*, 2012. "Measurement of frictional force characteristics of pneumatic cylinders under dry and lubricated conditions". *Przegląd Elektrotechniczny*, Vol. 88, No. 7b, pp. 261–264.

De Wit, C.C., Olsson, H., Astrom, K.J. and Lischinsky, P., 1995. "A new model for control of systems with friction". *IEEE Transactions on automatic control*, Vol. 40, No. 3, pp. 419–425.

Guenther, R., Perondi, E.A., DePieri, E.R. and Valdiero, A.C., 2006. "Cascade controlled pneumatic positioning system with lugre model based friction compensation". *Journal of the Brazilian Society of Mechanical Sciences and Engineering*, Vol. 28, No. 1, pp. 48–57.

Ha, J.L., Fung, R.F., Han, C.F. and Chang, J.R., 2006. "Effects of frictional models on the dynamic response of the impact drive mechanism". *Journal of vibration and acoustics*, Vol. 128, No. 1, pp. 88–96.

Johanastrom, K. and Canudas-de Wit, C., 2008. "Revisiting the lugre friction model". *IEEE control Systems*, Vol. 28, No. 6, pp. 101–114.

Nouri, B.M., 2004. "Friction identification in mechatronic systems". *ISA transactions*, Vol. 43, No. 2, pp. 205–216.
Perondi, E.A. *et al.*, 2002. "Controle não-linear em cascata de um servoposicionador pneumático com compensação do atrito".
Schroeder, L.E. and Singh, R., 1993. "Experimental study of friction in a pneumatic actuator at constant velocity". *Journal of dynamic systems, measurement, and control*, Vol. 115, No. 3, pp. 575–577.
Sun, Y.H., Chen, T., Wu, C.Q. and Shafai, C., 2016. "Comparison of four friction models: Feature prediction". *Journal of Computational and Nonlinear Dynamics*, Vol. 11, No. 3, p. 031009.

8. RESPONSIBILITY NOTICE

The authors are the only responsible for the printed material included in this paper.